Vishwakarma, B. D., Bates, P. D., Sneeuw, N., Westaway, R. M., & Bamber, J. L. (Accepted/In press). Re-assessing global water storage trends from GRACE time series. *Environmental Research Letters*. https://doi.org/10.1088/1748-9326/abd4a9

IOP Publishing Environmental Research Letters
Journal **XX** (XXXX) XXXXXX https://doi.org/XXXX/XXXX

Re-assessing global water storage trends from GRACE time series

B. D. Vishwakarma[1], P. Bates[1], N. Sneeuw[2], R. M. Westaway[1], and J. L. Bamber[1]

[1]School of Geographical Sciences, University of Bristol, Bristol, UK.

[2] Institute of Geodesy, University of Stuttgart, Stuttgart, Germany.

E-mail: bd.vishwakarma@bristol.ac.uk

Received xxxxxx
Accepted for publication xxxxxx
Published xxxxxx

Abstract

Monitoring changes in freshwater availability is critical for human society and sustainable economic development. To identify regions experiencing secular change in their water resources, many studies compute linear trends in the Total Water Storage (TWS) anomaly derived from the Gravity Recovery And Climate Experiment (GRACE) mission data. Such analyses suggest that several major water systems are under stress (1-6)**.**

TWS varies in space and time due to low frequency natural variability, anthropogenic intervention, and climate-change (7, 8)**. Therefore, linear trends from a short time series can only be interpreted in a meaningful way after accounting for natural spatiotemporal variability in TWS** (9, 10)**. In this study, we first show that GRACE TWS trends from a short time series cannot determine conclusively if an observed change is unprecedented or severe. To address this limitation, we develop a novel metric, Trend to Variability Ratio (TVR), that assesses the severity of TWS trends observed by GRACE from 2003–2015 relative to the multi-decadal climate-driven variability. We demonstrate that the TVR combined with the trend provides a more informative and complete assessment of water storage change. We show that similar trends imply markedly different severity of TWS change, depending on location. Currently more than 3.2 billion people are living in regions facing severe water storage depletion w.r.t past decades. Furthermore, nearly 36% of hydrological catchments losing water in the last decade have suffered from unprecedented loss. Inferences from this study can better inform water resource management.**

Keywords: GRACE, linear trends, spatiotemporal variability

1. Introduction

The total amount of rainfall received by a river system and its spatial variability depends on the climate zone(s) through which it flows (11). Precipitation also has a temporal variability dominated by an annual cycle that moves approximately 6000 ± 1400 Gt of water every year between land and oceans (12). On multi-annual timescales this water movement is primarily driven by ocean-atmosphere interactions characterized by climate indices such as the El Niño-Southern Oscillation (ENSO), North Atlantic Oscillations (NAO) or Atlantic Multidecadal Variability (AMV) (8, 13, 14). Interannual variability, operating at sub- to multi-decadal timescales, is responsible for unusual

precipitation that can lead to floods and droughts. Since precipitation is related to water storage change via the water budget equation, Total Water Storage (TWS) exhibits similar sub- to multi-decadal temporal variability (7, 14, 15). TWS is defined as the sum of water stored near the surface of the Earth in the form of soil moisture, snow water equivalent, surface water, canopy water storage, frozen reservoirs and groundwater aquifers (16, 17).

Understanding the cause and effect of spatiotemporal variability in TWS is essential to our assessment of global water security. It is understood that changes in TWS are driven primarily by natural variability and human exploitation of water resources, and are also evolving due to anthropogenic climate change (13). Given natural variability and human intervention, the rate of depletion in TWS sometimes exceeds the rate of replenishment and *vice-versa*. However, if the rate of depletion exceeds the rate of natural replenishment for significantly longer than the characteristic timescale of natural variability, then the water body is likely to be under stress due to external secular forcing.

The amount of publicly-shared *in-situ* hydrological information is limited and often decreasing due to political and financial pressures (6, 16), making it a challenge to monitor global water-systems efficiently. A partial solution to this problem has been provided by recent developments in satellite remote sensing. In particular, the launch of the Gravity Recovery And Climate Experiment (GRACE) satellite mission in 2002 allowed global measurement of the TWS anomaly for the first time (18-20). GRACE data have since been used to identify and understand the dynamics of the hydrosphere, including groundwater depletion, shrinking glaciers and ocean mass change (18, 19). Typically, the TWS time series from several years of GRACE data is decomposed into a seasonal signal and a linear trend computed using least-squares regression. The magnitude of any negative trend is then used as a measure of the severity of water loss to identify and rank regions in order of water storage stress (5, 6, 16). There are two issues with this approach:

a) the GRACE satellite mission provides a relatively short time series of approximately 17 years, which, depending on the region and the time-period, can be dominated by either natural variability, human intervention or anthropogenic climate change (9, 21). Without knowledge of the amplitude and the characteristic timescales of individual sources of variability, it is impossible to determine the driver, and consequently the significance, of GRACE-derived trends.

b) in general, each region has a distinct natural interannual variability, of sub- to multi-decadal time scale, which means the same negative trend cannot be used to infer the same degree of TWS stress. In other words, the magnitude of the TWS trend alone is not a measure of its severity.

These issues are illustrated in Figure 1, where we plot natural variability in TWS from a calibrated Land Surface Model (LSM) and select three different time-periods (10, 7 and 13 years, respectively) in the latter half of the 20th century to infer a linear trend, while the trend for the complete time series from the calibrated LSM is negligible in each case. We can see that the natural variability for different catchments is different and even large trends from short time series (such as obtained from GRACE) might be driven by natural variability for some catchments. More details on the data and processing strategy used to generate Figure 1 – which is only for illustrative purposes – can be found in the supplementary information. To this end, we can conclude that a comprehensive assessment of the severity of TWS trends cannot be obtained from GRACE observations alone, and additional information on multi-decadal natural variability is needed. In this study we address this issue and develop a new metric that when used along trends can help us infer the severity of TWS change.

2. Trend to variability ratio

Determining when a trend exceeds the expected internal variability is a fundamental problem in many disciplines. Similar issues have been identified by studies concerning the emergence of climate change signal in Earth system model simulations where it is easier to separate internal variability by changing the initial condition and forcing (22, 23). For example, in the context of ocean heat content, a warming trend is only detectable from a time series longer than 27 years, while trends from shorter time series are likely dominated and contaminated by natural variability (24). By normalizing the trend against the standard deviation of the internal variability, we can assess when the trend emerges above the system's natural variability. In this study we apply this basic idea to study the severity of TWS change by normalising TWS trends and devising a dimensionless metric to help quantify their magnitude relative to natural variability. We use the ratio between the total change, obtained by multiplying the overall TWS trend by the length of the time series, and 1 σ of natural interannual variability. We call this metric the Trend to Variability Ratio (TVR), written as

$\mathrm{TVR} = \frac{t \cdot n}{\sigma}$.

In the context of TWS, the numerator represents the TWS change in n years with a trend t given in mm/yr, the denominator σ is the standard deviation (in mm) of the multi-decadal natural interannual variability. A TVR between $+2$ and -2 means that the TWS change is within the 90th percentile (5-95th percentile for a Gaussian distribution) expected range due to multi-decadal natural variability and the trend is not exceptional. If the TVR is between -2 and -3 or $+2$ and $+3$, the region is experiencing an extreme event albeit one that it has likely experienced in the past and lies within approximately 98% credible range. However, if the TVR exceeds ± 3, the TWS change can be considered exceptional and unlikely to have been experienced in the recent past. Therefore, TVR along with trends can help us assess the severity of ongoing TWS change in the context of previous decades, which is imperative for developing policy for countering likely water-stress in the near future. Time of emergence studies focus on estimating when the secular signal will surpass the natural variability, while we are focusing on understanding the severity of trends from short GRACE time series in context of past TWS natural variability. Therefore, TVR is not a statistical significance metric like R^2, Spearman's rho test, Mann-Kendall test, or Innovative trend analysis method (25), but a tool to put the trend from a short observation time series in the context of past natural variability.

3. Natural TWS variability

A key challenge of this approach is to obtain an estimate of natural interannual variability of the TWS anomaly from a multi-decadal time series that adequately captures long-term TWS behaviour. One option is to use output from global numerical models that simulate multi-decadal time series of various components of TWS. These global hydrology models can be categorized into Land Surface-hydrology Models (LSMs), such as the Global Land Data Assimilation System (GLDAS) Noah, and Global Hydrological and Water Resource Models (WGHRMs), such as the WaterGap Hydrological Model and PCR-GLOBWB. LSMs exclude natural groundwater cycles and are poorly constrained in data-sparse regions, resulting in large uncertainties that vary in space and time (26), while WGHRMs include groundwater storage and estimates of human abstractions making it hard to use model estimates as a representative of natural variability alone. Furthermore, it has been shown that both types of global hydrological models tend to underestimate trends in TWS (27). Therefore, outputs from these state-of-the-art are not the best representation of natural inter-annual variability. For this reason, we use a novel statistical model output, GRACE-REC, that has been shown to capture climate driven TWS interannual variations with good accuracy (28). GRACE-REC time series have been shown to perform better than the state-of-the-art models when tested against independent evaluation datasets such as the sea level budget, large-scale water balance from atmospheric reanalysis, and in situ streamflow measurements.

GRACE-REC is generated by a statistical model that uses meteorological data, such as precipitation and surface temperature, as input and is trained by GRACE observations to reconstruct past TWS anomalies. The model is calibrated using GRACE time series but with the linear trend and seasonal signal removed, which helps eliminate anthropogenic signals and emphasise inter-annual variability to a large extent (28). The model efficacy has been shown to be of poor quality for a few grid cells (such as central Asia, North Africa) (28), but at catchment scale the efficacy would be better. The model output is available from 1901 to mid-2019, providing a long time series. The statistical model has six variants that arise from choice of using training data from two GRACE processing centers and three meteorological forcing time series. Thus GRACE-REC provides six reconstructions of interannual TWS time series and each reconstruction has 100 ensemble members. Since some meteorological forcing datasets such as MSWEP and ERA5 are only available from 1979 onwards, four GRACE-REC reconstructions start from 1979. We thus compute the mean from all 100 ensemble members of six GRACE-REC reconstructions from 1979 to 2019, providing us with a robust estimate of climate-driven interannual TWS over the last four decades. We note that the efficacy of GRACE-REC is low in some areas, such as Highland of Tibet, Saudi Arabia, and Northern Sahara (28). Therefore, we have not computed TVR over these regions. Nevertheless, for readers interested in these regions, we provide an additional TVR plot in supplementary information Figure S1.

4. GRACE time series

The TWS time series from GRACE is decomposed using STL (Seasonal and Trend decomposition using LOESS) to obtain an annual and interannual signal (29). The climate-driven interannual time series from GRACE-REC, referred to from here on as the normal TWS variability, is assumed to be free from a direct human intervention signal. Figure 2 (b) shows the standard deviation of the normal TWS variability for 3° grid cells, and Figure 3(b) shows the same metric by river catchment. It is evident that normal TWS variability varies markedly from one catchment to another, by as much as a factor 10. The interannual signal consists of long wavelength signal (year to year variations including the trend signal). Therefore, trend over a given period is obtained from a linear fit to the interannual signal. Please note that GRACE trends can be assumed to represent TWS change when other signals, such as tectonics and GIA in glaciated regions, have been accurately taken care of. Hence, TWS trends might be affected by residual tectonic effects and GIA signal in glaciated regions and by post-seismic signals in regions affected by large Earthquakes. Therefore, reader's discretion is required. Furthermore, GRACE products are known to have a coarse spatial resolution that is approximately 3° (30), thus they are more accurate when used for catchment-scale analysis. It has been shown that the accuracy of GRACE time series improves as the catchment area increases (31). Therefore, we analyse GRACE products at two spatial scales: at a global 3° grid-scale and at a catchment-scale. We study 160 catchments that are larger than the minimum recommended area of approximately 65,000 km^2 (31). The catchment-scale results are important for understanding the health of river systems, while grid-scale results help identify spatial variability within catchments and other regions.

5. Results

We subsequently calculate and plot TVR at both the grid-scale (Figure 2(c)) and catchment-scale (Figure 4). Figure 4 also serves to illustrate the concept. The uncertainty in TVR is shown in supplementary Figure S2. The TVR plots inform us about the severity of the GRACE trend signal with respect to the last four decades of hydrological variability. Looking at the TWS trend maps (Figure 2(a) or Figure 3(a)) alongside the corresponding TVR map (Figure 2(c) or Figure 4), we can see that Alaska, the Caspian Sea, Northern India, Argentina, Chile, the Eastern Amazon, the High Plains Aquifer and California are hotspots of TWS loss. The drivers for the trends in these regions have been investigated and discussed previously (1-6, 16, 19): glaciers are losing mass in Alaska;

the Caspian Sea is losing water at an unprecedented rate; Northern India, California and the High Plains Aquifer are experiencing unprecedented groundwater abstraction; and Argentina, Chile and the Eastern Amazon all suffered from drought in the last decade. Introducing the TVR alongside the TWS trend additionally reveals that Iran, North-East China, Kazakhstan, South-East Asia, and several catchments in Southern Africa are also experiencing abnormal TWS loss. Furthermore, the TVR also helps us to assess the relative stress between two catchments in a quantitative manner. In Supplementary Table 1 we list all the catchments with a negative TWS trend in order of decreasing magnitude and their respective TVR. This rank order changes considerably if we choose TVR as the metric for water storage stress instead of the TWS trend value. This is further demonstrated in Figure 5, where we have plotted the relationship between the ranked order of the catchments when sorted by trend versus when sorted by TVR. If TVR offers no additional information, the points would have a 1:1 relationship and fall on the diagonal; yet as Figure 5 shows there are substantial deviations. Taking an arbitrary threshold of ±20 in rank change, we have highlighted those regions and catchments that would be categorised significantly different when using TVR instead of trend magnitude. Blue dots in the figure represent less sever TWS change compared to that perceived by trend magnitude while red dot represent more sever TWS change. For example, the Colorado river in Argentina and the Jequitinhonha river catchment in Brazil both have a strong negative TWS trend of around -18.8 mm/yr, but the TVR of the Colorado river basin (-5.7) suggests a severe and exceptional water loss and is much higher than that of the Jequitinhonha basin (-1.6). This finding is supported by research discussing the major drought event between 2010 and 2015 in the central Andes in Argentina (32), with no similar events reported for the GRACE period in the Jequitinhonha river catchment.

On a continental scale, the TVR metric indicates that there is more water stress in Asia than would be inferred from TWS trends alone (6, 16). For example, the Tigris river basin in Iraq has a TWS trend of -18 mm/yr and a TVR of -3.4, which suggests an exceptional water loss in the region due to recent droughts and anthropogenic water exploitation in the middle-East (33, 34). River catchments in Iran have a negative TWS trend and large TVR value (the Zagros, South Iran, and Karun river catchments with TWS trends of -22.6, -8.9, -16.3 mm/yr and a TVR of -11.1, -6.9, and -3.9 respectively), suggesting severe TWS loss, which is supported by research that reports that Iran lost water at a rate of 25 ± 3 Gt/yr between 2003 and 2012, of which 14 ±3 Gt/yr (56%) was found to be anthropogenic (33). Similarly, the Brahmaputra has a negative TWS trend value (-14 mm/yr), lower than both the Tigris and Colorado, but its TVR (-13.3) suggests that it is experiencing an exceptional change, which is primarily driven by a steep and unprecedented decrease in rainfall over the last decade that has been attributed to anthropogenic climate change (6, 35). The Yellow River in China has a small trend of -4.2 mm/yr but its TVR is -3.7, while the Volga River in Russia has a trend of -5.1 mm/yr and a TVR of -2. The Brazos, Ganges, and Yukon rivers have a strong linear trend of approximately -12 mm/yr but a TVR of -3.2, -4.2, and -8.0 respectively.

TVR normalizes the global TWS trend map with respect to the natural variability, which identify regions experiencing abnormal and severe TWS change irrespective of their TWS trend magnitude. For example, the TVR map shows that densely populated regions of the Indian subcontinent are experiencing exceptional TWS loss, which is supported by recent reports (36). In 2018, a planning body of the Government of India reported that 600 million people in India are facing severe water stress and approximately 200,000 people die every year due to inadequate access to safe water (36). It is projected that by 2030 the water demand in India will double owing to population rise and economic development (36). Currently more than 1.4 billion people depend on water from the Indus, Ganges, Brahmaputra, Yangtze, and Yellow rivers (37). We find that all these rivers, except for the Yangtze, are experiencing abnormal TWS

decline. We use population data provided by the Socioeconomic Data and Applications Center (SEDAC) (38) and the global grid-scale TVR map to estimate that in 2015 more than 3.2 billion people worldwide (~43% of the total global population) were living in regions experiencing severe decreasing TWS trends, i.e. with a TVR less than −3. Therefore, strict and urgent measures are required to avoid a profound and pervasive water crisis in the future.

Conversely, several catchments have a strongly positive TVR. Anthropogenic climate change and direct human intervention (e.g. water impoundment) may be the reasons behind such a net positive change. For example, the Yangtze river has shown a strong positive TWS trend due to the filling up of the Three Gorges and other reservoirs (6, 39), which explains a TVR of +2.2 despite a weakly positive TWS trend of +2.6 mm/yr. Similarly, the Zambezi (TVR = +2.6), Volta (+4.6), Okavango (+4.4) and Niger (+4) catchments in Africa, and the Amazon (+2.4) catchment in South America all exhibit an increase in TWS and a positive TVR, which can largely be explained by an intensifying water cycle due to anthropogenic climate change (13, 40, 41).

From these results, it is clear that many catchments with similar TWS trends have markedly different TVR values, including many river catchments that have a moderate negative TWS trends but that are revealed to be losing water at an exceptional rate after accounting for natural variability, and vice versa.

We conclude that using TVR provides a complementary and meaningful metric for assessing the severity of TWS trends. The GRACE mission, decommissioned in 2017, has provided unique insights into global TWS variability over the last 15 years. The successful launch of the GRACE-Follow-On mission in May 2018 offers the potential to continue the global observational record of TWS for another decade or more. This provides us with an opportunity to track global water storage stress and inform water-management decisions and policy for sustainable development. Until GRACE observations provide longer time series, GRACE TWS trends alone cannot definitively evaluate the severity of TWS loss or gain, and the use of the TVR metric allows for a more informative interpretation of the trends. We further believe that the concept behind the TVR can benefit other disciplines that rely on signal detection and trend analysis from relatively short time series.

Table 1. List of selected catchments with (a) TVR ≤ -3 or (b) TVR >+3, sorted by TVR. Catchments with small TWS trends (TWS trend <-5 or TWS trend >+5, respectively) but with high TVR (i.e. those unlikely to be identified as having severe water loss or water abundance using TWS trend alone) are highlighted.

(a)

Catchment Name	Trends (mm/yr)	TVR (dimensionless)
Caspian Sea	-20.4 ± 1	-15.7 ± 0.8
Brahmaputra	-14 ± 1.7	-13.3 ± 1.6
Zagros (Iran)	-22.6 ± 3.9	-11.1 ± 1.9
Copper River	-60.7 ± 2.6	-8.8 ± 0.4
Kura	-18.7 ± 1.8	-8.8 ± 0.9
Yukon River	-12.2 ± 1.2	-8 ± 0.8
Thelon River	-8.6 ± 1.5	-7.1 ± 1.2
South Iran	-8.9 ± 1.6	-6.9 ± 1.3
Churchill	-9 ± 1.9	-6.1 ± 1.3
Colorado (Argentina)	-18.9 ± 2.3	-5.7 ± 0.7
Kuskokwim River	-13.8 ± 2.2	-5.7 ± 0.9
Negro (Argentina)	-13.8 ± 2.5	-5.1 ± 0.9
Luan He	-8.4 ± 1.6	-4.6 ± 0.9
Huai He	-13.7 ± 4.7	-4.3 ± 1.4
Ganges	-12.1 ± 2.5	-4.2 ± 0.9
Indus	-7.6 ± 1.9	-4.1 ± 1
Karun	-16.3 ± 3	-3.9 ± 0.7
Mackenzie River	-3.7 ± 1	-3.9 ± 1
Salado	-13.7 ± 3.3	-3.7 ± 0.9

Colorado River (Caribbean)	-11.9 ± 2.6	-3.7 ± 0.8
Irrawaddy	-8.3 ± 2.4	-3.7 ± 1.1
Yellow River	-4.3 ± 1.3	-3.7 ± 1.1
Argentina	-14.3 ± 3.2	-3.6 ± 0.8
Fraser River	-10.6 ± 2.4	-3.3 ± 0.7
Brazos River	-12.3 ± 2.9	-3.2 ± 0.7
Aral Sea	-3.9 ± 0.9	-3.1 ± 0.7
Gobi	-1.2 ± 0.6	-3.1 ± 1.7
Tigris	-18 ± 3.9	-3.4 ± 0.7
Don	-12.5 ± 1.7	-3 ± 0.4
Euphrates	-11 ± 2.1	-3.7 ± 0.7
Atacama	-3.4 ± 2.2	-3 ± 1.9

(b)

Catchment Name	**Trends (mm/yr)**	**TVR (dimensionless)**
Niger	5 ± 1.1	6.8 ± 1.5
Saguenay	7.9 ± 2.1	5.7 ± 1.5
Nottaway	7.8 ± 2.1	5.2 ± 1.4
Nelson River	11.9 ± 1.6	4.7 ± 0.6
Volta	11.1 ± 2.2	4.6 ± 0.9
Okavango	12.4 ± 2.3	4.4 ± 0.8
St.Lawrence	8.5 ± 1.5	3.5 ± 0.6
Moose River	7.5 ± 2	3.3 ± 0.9
Nile	3 ± 1.2	3.3 ± 1.3
Sanaga	2.1 ± 2.5	3.3 ± 3.9
Comoe	9.3 ± 2.2	3.2 ± 0.8

Acknowledgements

BDV is supported by the Marie Skłodowska-Curie Individual Fellowship (MSCA-IF) under Grant Agreement 841407 (CLOSeR). JB, PB and RW are supported by the European Research Council (ERC) under the European Union's Horizon 2020 research + innovation program, under grant agreement no 694188 (GlobalMass project). PB is also supported by a Royal Society Wolfson Research Merit Award. We would like to thank Prof. Jonathan Rougier for his insightful comments and discussions.

Data availability

The data used in this study are available free of cost from various sources: the GRACE spherical harmonic coefficients used were downloaded from ftp://ftp.tugraz.at/outgoing/ITSG/GRACE/ITSG-Grace2016/monthly/monthly_n90, accessed on 05 September 2017. We have made use of C_{20} and degree 1 spherical harmonic coefficients available at grace.jpl.nasa.gov accessed on 10 September 2017, and catchment boundaries available at http://www.bafg.de/GRDC/EN/02srvcs/22gslrs/221MRB/riverbasinsnode.html, accessed on 30 September 2016. The GIA ICE-6GD model data was downloaded from http://www.atmosp.physics.utoronto.ca/~peltier/data.php on 08 February 2018. GRACE JPL Mascon data are available at http://grace.jpl.nasa.gov, supported by the NASA MEaSUREs Program, accessed on 05 February 2019. The GRACE-REC time series were accessed on 25 September 2019 from https://figshare.com/articles/GRACE-REC_A_reconstruction_of_climate-driven_water_storage_changes_over_the_last_century/7670849.

Code availability

MATLAB scripts for obtaining data-driven leakage corrected GRACE TWS time series at catchment scale are freely available at https://www.gis.uni-stuttgart.de/en/research/downloads/. The MATLAB script to process GRACE-REC data, include GIA adjustments to GRACE time series, time series analyses and TVR computation will be made available by BDV upon reasonable request.

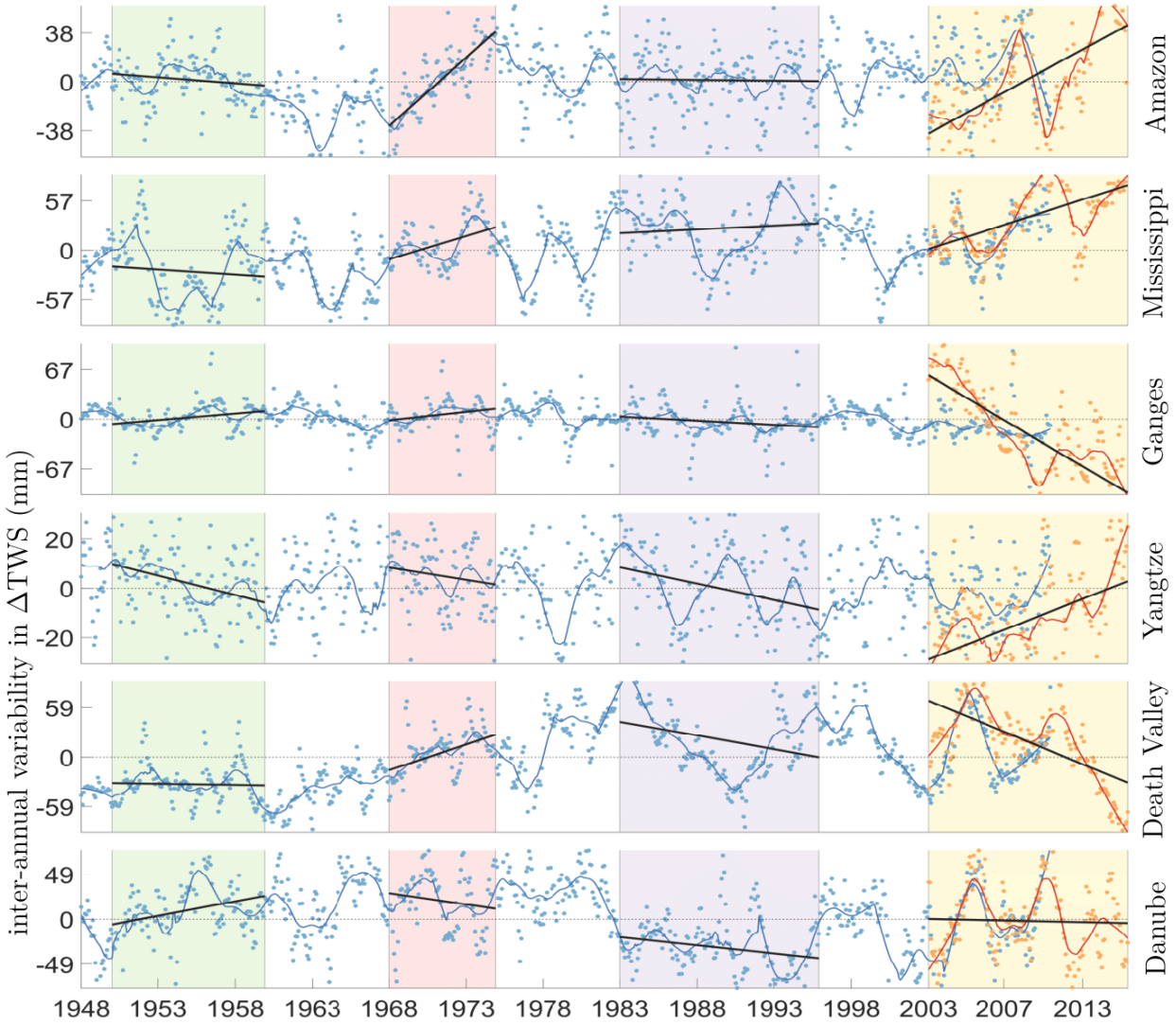

Figure 1: Interannual TWS time series for six different river catchments from GLDAS model output (blue dots and line) and GRACE data (orange dots and red line). Dots represent the signal after removing the dominant annual signal from the time series and the lines represent the LOESS fit. The linear trend from the interannual signal for four time periods is shown by the black lines and they have been shaded (colours chosen arbitrarily) to highlight how short time series can suggest markedly different, and in some cases misleading, TWS trends.

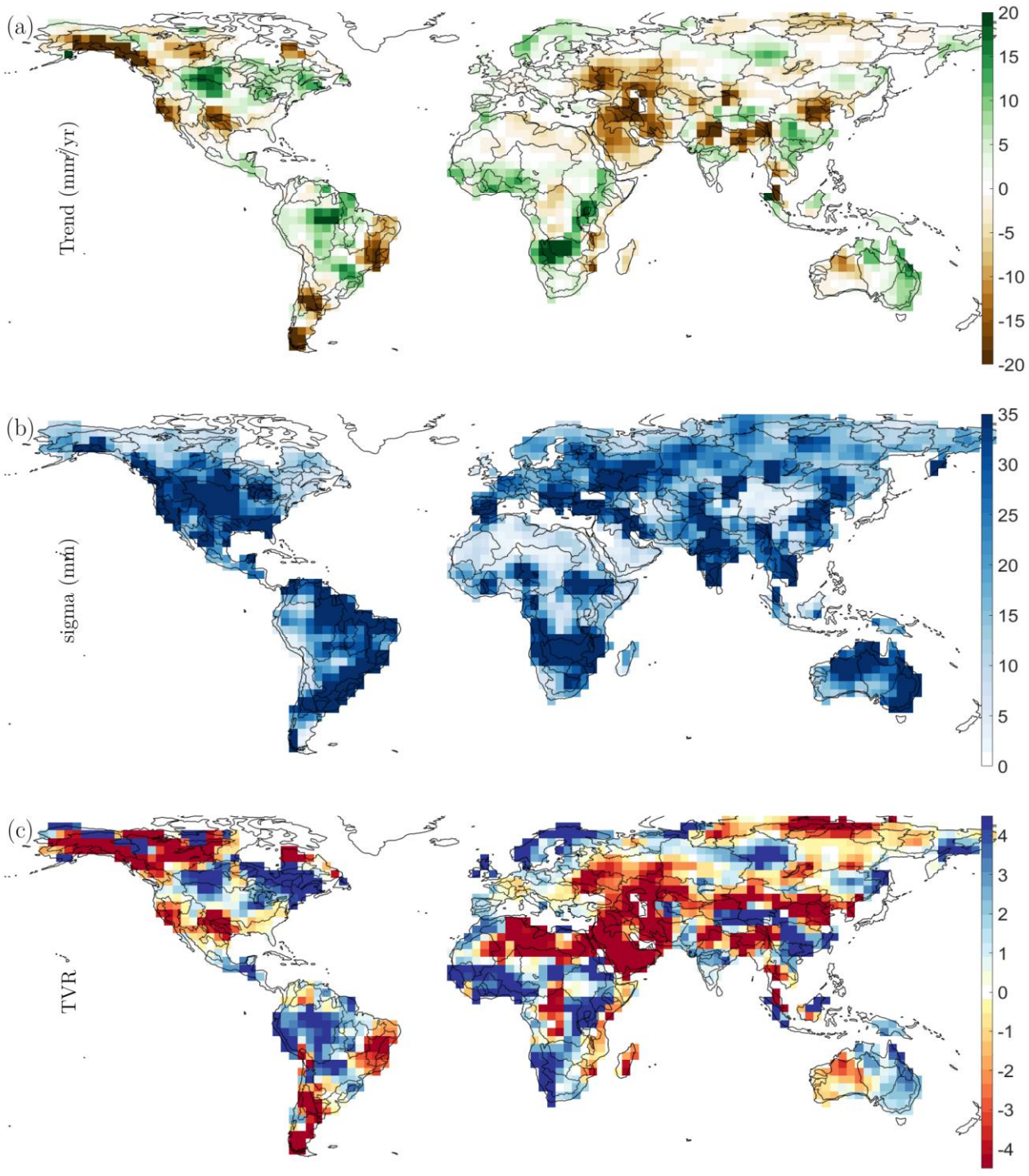

Figure 2: (a) Maps of 3° gridded JPL release 06 mascon trends, (b) standard deviation of GRACE-REC at 3° grid resolution, and (c) the grid-scale TVR map.

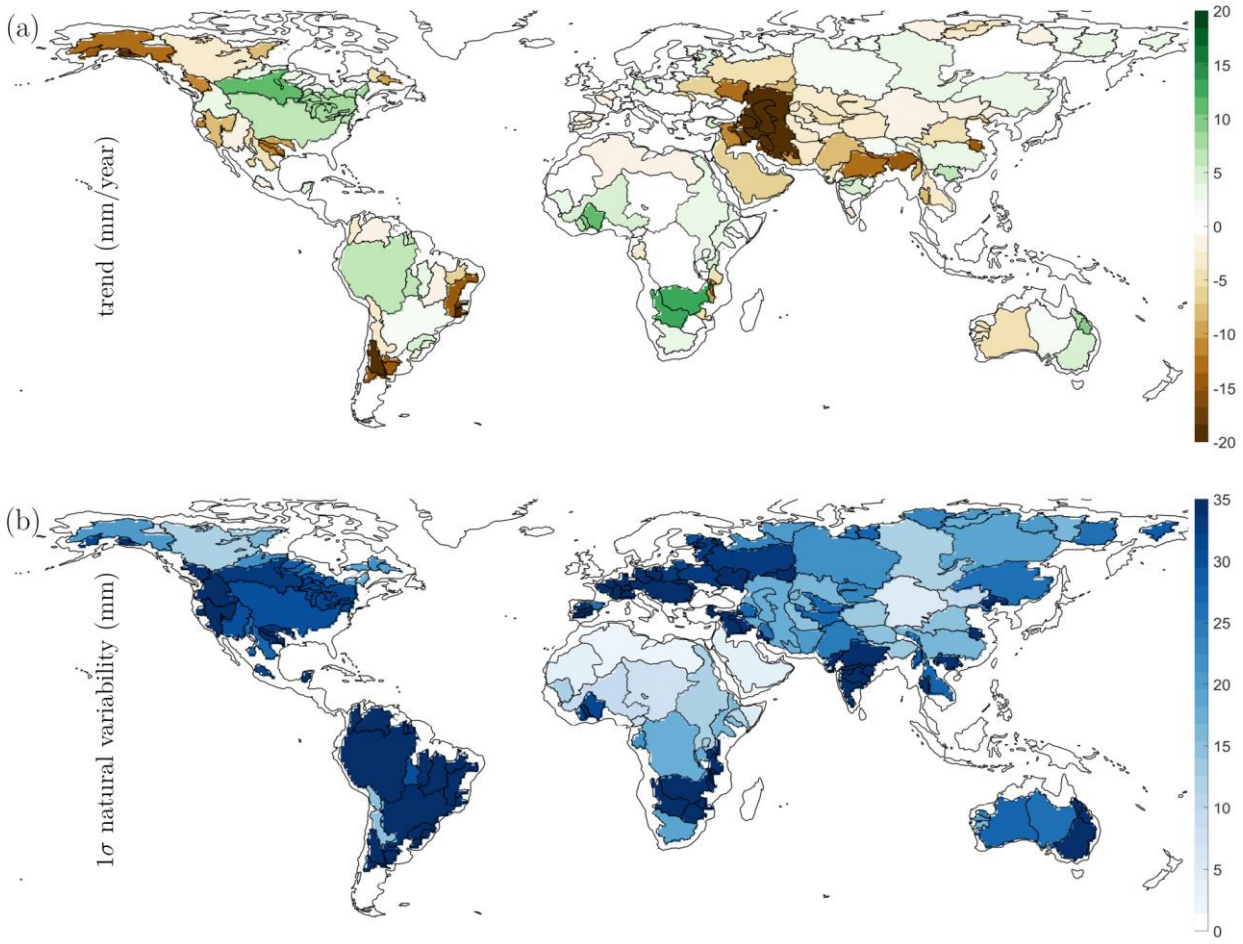

Figure 3: (a) Linear TWS trend signal from GRACE fields; (b) standard deviation of TWS interannual variability from GRACE-REC.

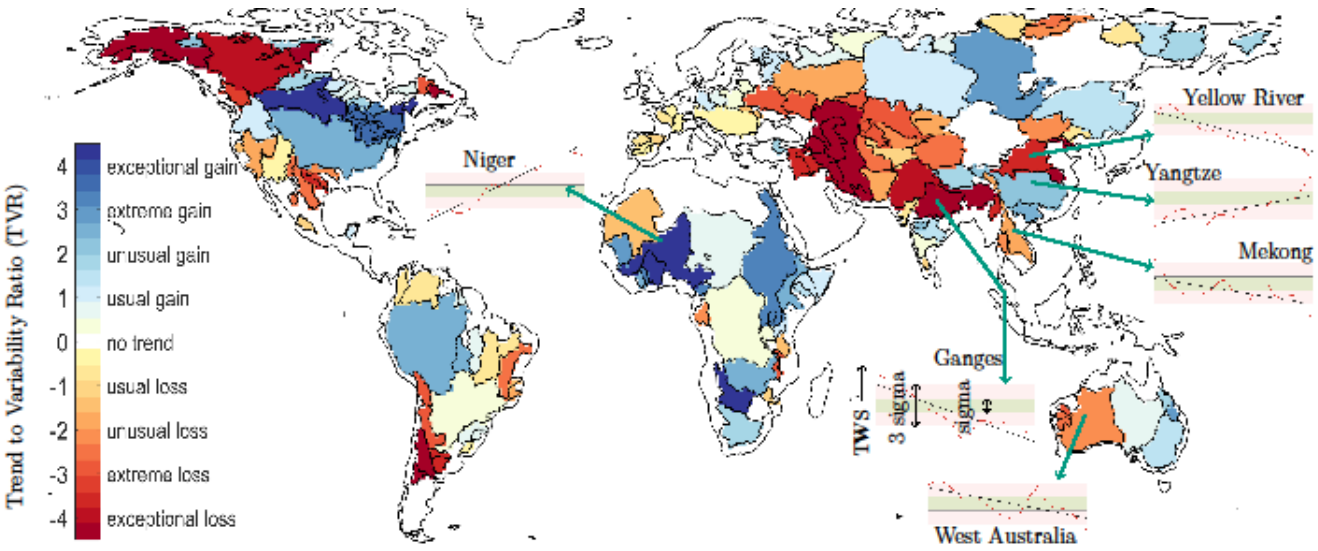

Figure 4: Catchment-scale TVR for the 160 catchments investigated. Inset time series plots are shown to illustrate the method for seven river catchments. In these, the green and pink bands represent the 1- and 3-sigma of the normal TWS variability, respectively. Catchments that exceed the normal TWS variability of 3-sigma have a TVR value that suggests exceptional change.

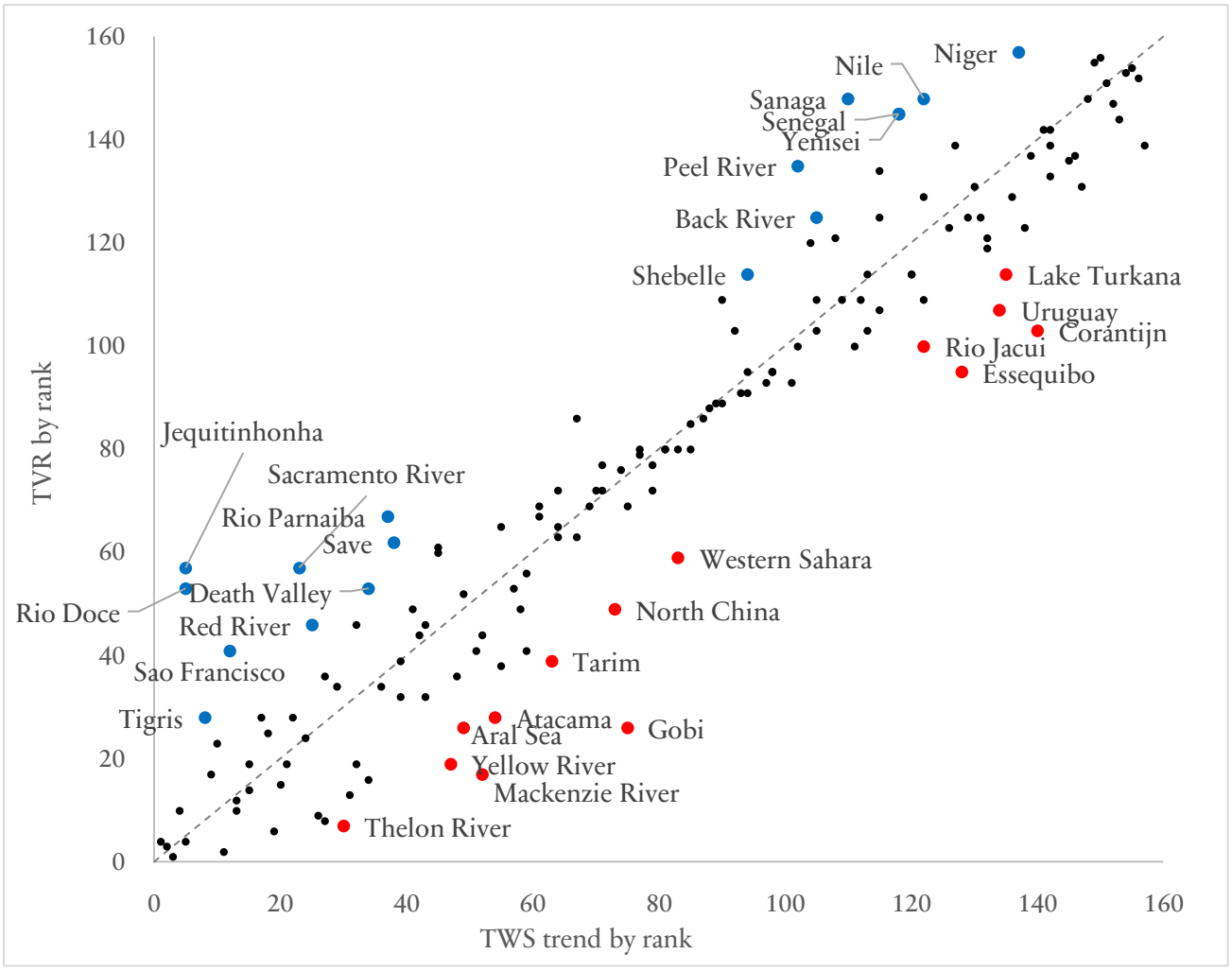

Figure 5: Scatter plot between catchment rank order when sorted by trend value and when sorted by TVR. If TVR adds no additional information all the catchments would lie on the diagonal. Catchment whose rank changes by more than 20 (arbitrary threshold) are highlighted as blue or red dots. Red (blue) dots represent those catchments and regions where TVR suggests that TWS change is more (less) alarming compared to inferences from trends.

References

1. Rodell M, Velicogna I, Famiglietti JS. Satellite-based estimates of groundwater depletion in India. nature. 2009;460(7258):999–1002.
2. Long D, Scanlon BR, Longuevergne L, Sun AY, Fernando DN, Save H. GRACE satellite monitoring of large depletion in water storage in response to the 2011 drought in Texas. Geophys Res Lett. 2013;40(13):3395-401.
3. Richey AS, Thomas BF, Lo MH, Reager JT, Famiglietti JS, Voss K, et al. Quantifying renewable groundwater stress with GRACE. Water Resour Res. 2015;51(7):5217-38.
4. Voss KA, Famiglietti JS, Lo MH, de Linage C, Rodell M, Swenson SC. Groundwater depletion in the Middle East from GRACE with implications for transboundary water management in the Tigris-Euphrates-Western Iran region. Water Resour Res. 2013;49(2):904-14.
5. Famiglietti JS. The global groundwater crisis. Nature Climate Change. 2014;4(19):945–8.

6. Rodell M, Famiglietti JS, Wiese DN, Reager JT, Beaudoing HK, Landerer FW, et al. Emerging trends in global freshwater availability. nature. 2018;557:651 – 9.
7. Hamlington BD, Reager JT, Lo M-H, Karnauskas KB, Leben RR. Separating decadal global water cycle variability from sea level rise. Scientific Reports. 2017;7(24):995.
8. Nerem RS, Beckley BD, Fasullo JT, Hamlington BD, Masters D, Mitchum GT. Climate-change driven accelerated sea-level rise detected in the altimeter era. Proceedings of the National Academy of Sciences. 2018.
9. Paolo FS, Fricker HA, Padman L. Volume loss from Antarctic ice shelves is accelerating. Science. 2015;348(6232):327–31.
10. Edward H, R S. Time of emergence of climate signals. Geophysical Research Letters. 2012;39(1):L01702.
11. Koppen W. The thermal zones of the Earth according to the duration of hot, moderate and cold periods and to the impact of heat on the organic world. Meteorol Z. 2011;20(3):351-60.
12. Reager JT, Gardner AS, Famiglietti JS, Wiese DN, Eicker A, Lo MH. A decade of sea level rise slowed by climate-driven hydrology. Science. 2016;351(6274):699-703.
13. Eicker A, Forootan E, Springer A, Longuevergne L, Kusche J. Does GRACE see the terrestrial water cycle "intensifying"? Journal of Geophysical Research-Atmospheres. 2016;121(2):733-45.
14. Latif M, Keenlyside NS. A perspective on decadal climate variability and predictability. Deep-Sea Research Part II-Topical Studies in Oceanography. 2011;58(17-18):1880-94.
15. Beaudoing H, Rodell M. GLDAS Noah Land Surface Model L4 monthly 1.0 x 1.0 degree V2.0. Website, Goddard Earth Sciences Data and Information Services Center (GES DISC); 2015.
16. Chen J, Famiglietti JS, Scanlon BR, Rodell M. Groundwater Storage Changes: Present Status from GRACE Observations. Surveys in Geophysics. 2016;37(2):397–417.
17. Lorenz C, Devaraju B, Tourian MJ, Sneeuw N, Riegger J, Kunstmann H. Large-scale runoff from landmasses: a global assessment of the closure of the hydrological and atmospheric water balances. Journal of Hydrometeorology. 2014;15:2111–39.
18. Ramillien G, Famiglietti JS, Wahr J. Detection of Continental Hydrology and Glaciology Signals from GRACE: A Review. Surveys in Geophysics. 2008;29(4-5):361–74.
19. Wouters B, Bonin JA, Chambers DP, Riva REM, Sasgen I, Wahr J. GRACE, time-varying gravity, Earth system dynamics and climate change. Reports on Progress in Physics. 2014;77(11):116801.
20. Vishwakarma BD, Horwath M, Devaraju B, Groh A, Sneeuw N. A Data-Driven Approach for Repairing the Hydrological Catchment Signal Damage Due to Filtering of GRACE Products. Water Resources Research. 2017;53(11):9824-44.
21. Wouters B, Bamber JL, van den Broeke, R. M, Lenaerts JTM, Sasgen I. Limits in detecting acceleration of ice sheet mass loss due to climate variability. Nature Geoscience. 2011;6:613.
22. McKinnon KA, Deser C. Internal Variability and Regional Climate Trends in an Observational Large Ensemble. Journal of Climate. 2018;31(17):6783-802.
23. Deser C, Phillips AS, Simpson IR, Rosenbloom N, Coleman D, Lehner F, et al. Isolating the Evolving Contributions of Anthropogenic Aerosols and Greenhouse Gases: A New CESM1 Large Ensemble Community Resource. Journal of Climate. 2020;33(18):7835-58.
24. Cheng LJ, Trenberth KE, Fasullo J, Boyer T, Abraham J, Zhu J. Improved estimates of ocean heat content from 1960 to 2015. Sci Adv. 2017;3(3).
25. Şen Z. Innovative Trend Analysis Methodology. Journal of Hydrologic Engineering. 2012;17(9):1042-6.
26. Scanlon BR, Zhang Z, Save H, Sun AY, Mueller Schmied H, van Beek LPH, et al. Global models underestimate large decadal declining and rising water storage trends relative to GRACE satellite data. Proceedings of the National Academy of Sciences. 2018;115((6)):E1080–E9.
27. Scanlon BR, Zhang Z, Save H, Sun AY, Muller Schmied H, van Beek LPH, et al. Global models underestimate large decadal declining and rising water storage trends relative to GRACE satellite data. Proceedings of the National Academy of Sciences of the United States of America. 2018;115(6):E1080-E9.
28. Humphrey V, Gudmundsson L. GRACE-REC: a reconstruction of climate-driven water storage changes over the last century. Earth Syst Sci Data. 2019;11(3):1153-70.
29. Cleveland R, Cleveland W, McRae J, Terpenning I. STL: A Seasonal-Trend Decomposition Procedure Based on Loess (with Discussion). Journal of Official Statistics. 1990;6:3–73.
30. Watkins MM, Wiese DN, Yuan DN, Boening C, Landerer FW. Improved methods for observing Earth's time variable mass distribution with GRACE using spherical cap mascons. Journal of Geophysical Research-Solid Earth. 2015;120(4):2648-71.
31. Vishwakarma BD, Devaraju B, Sneeuw N. What Is the Spatial Resolution of GRACE Satellite Products for Hydrology? Remote Sensing. 2018;10(6).
32. Rivera JA, Penalba OC, Villalba R, Araneo DC. Spatio-Temporal Patterns of the 2010-2015 Extreme Hydrological Drought across the Central Andes, Argentina. Water-Sui. 2017;9(9).
33. Joodaki G, Wahr J, Swenson S. Estimating the human contribution to groundwater depletion in the Middle East, from GRACE data, land surface models, and well observations. Water Resources Research. 2014;50(3):2679-92.
34. Forootan E, Rietbroek R, Kusche J, Sharifi MA, Awange JL, Schmidt M, et al. Separation of large scale water storage patterns over Iran using GRACE, altimetry and hydrological data. Remote Sensing of Environment. 2014;140:580 – 95.
35. Deka RL, Mahanta C, Pathak H, Nath KK, Das S. Trends and fluctuations of rainfall regime in the Brahmaputra

and Barak basins of Assam, India. Theoretical and Applied Climatology. 2013;114(1):61–71.

36. NITI, Aayog, team. Composite water management index: a tool for water management. Report. National Institution for Transforming India, Government of India; 2018 June.

37. Immerzeel WW, van Beek LPH, Bierkens MFP. Climate Change Will Affect the Asian Water Towers. Science. 2010;328(5984):1382–5.

38. CIESIN. Gridded Population of the World, Version 3 (GPWv3): Population Count Grid, Future Estimates. NASA Socioeconomic Data and Applications Center (SEDAC); 2005.

39. Wang X, de Linage C, Famiglietti J, Zender CS. Gravity Recovery and Climate Experiment (GRACE) detection of water storage changes in the Three Gorges Reservoir of China and comparison with in situ measurements. Water Resources Research. 2011;47(12):W12502.

40. Wang XY, Li XC, Zhu J, Tanajura CAS. The strengthening of Amazonian precipitation during the wet season driven by tropical sea surface temperature forcing. Environmental Research Letters. 2018;13(9).

41. Hassan A, Jin SG. Water storage changes and balances in Africa observed by GRACE and hydrologic models. Geodesy and Geodynamics. 2016;7(1):39-49.